The RanBP2/RanGAP1-SUMO complex gates β-arrestin2 nuclear entry to regulate the Mdm2-p53 signaling axis

Elodie Blondel-Tepaz, Marie Leverve, Badr Sokrat, Justine Paradis, Milena Kosic, Kusumika Saha, Cédric Auffray, Evelyne Lima-Fernandes, Alessia Zamborlini, Anne Poupon, et al.

The RanBP2/RanGAP1-SUMO complex gates β-arrestin2 nuclear entry to regulate the Mdm2-p53 signalling axis

Elodie Blondel-Tepaz[1,2,3], Marie Leverve[1,2,3], Badr Sokrat[4,5], Justine S. Paradis[5,6], Milena Kosic[7], Kusumika Saha[1,2,3], Cédric Auffray[1,2,3], Evelyne Lima-Fernandes[1,2,3], Alessia Zamborlini[8], Anne Poupon[9], Louis Gaboury[5,10], Jane Findlay[11], George S. Baillie[11], Hervé Enslen[1,2,3] Michel Bouvier[5,6], Stéphane Angers[7], Stefano Marullo[1,2,3] and Mark G.H. Scott[1,2,3,*]

[1]: Inserm, U1016, Institut Cochin, Paris, France
[2]: CNRS, UMR8104, Paris, France
[3]: Université de Paris
[4]: Institute for Research in Immunology and Cancer (IRIC), Université de Montréal, Montréal, Québec, Canada
[5]: Department of Biochemistry and Molecular Medicine, Université de Montréal, Montréal, Québec, Canada
[6]: Molecular Biology Program, Université de Montréal, Montréal, Québec, Canada
[7]: Leslie Dan Faculty of Pharmacy and Department of Biochemistry, University of Toronto, Toronto, Canada
[8]: Institute for Integrative Biology of the Cell (I2BC), CEA, CNRS, Université Paris-Saclay, France
[9]: PRC, INRA, CNRS, IFCE, Université de Tours, 37380 Nouzilly, France
[10]: Department of Pathology and Cell Biology, IRIC, Université de Montréal, Montréal, Québec, Canada
[11]: Institute of Cardiovascular and Medical Sciences, College of Veterinary, Medical and Life Sciences, University of Glasgow, Glasgow, UK

[*]Corresponding author:
mark.scott@inserm.fr

Address:
Institut Cochin, CNRS UMR8104, INSERM U1016, Université de Paris
27, Rue du Faubourg Saint Jacques, 75014 Paris, France

Running title: SUMO gates β-arr2 cytonuclear shuttling (39 characters)

Keywords: β-arrestin/Mdm2/p53/RanGAP1/SUMO

Abstract

Mdm2 antagonizes the tumour suppressor p53. Targeting the Mdm2-p53 interaction represents an attractive approach for the treatment of cancers with functional p53. Investigating mechanisms underlying Mdm2-p53 regulation is therefore important. The scaffold protein β-arrestin2 (β-arr2) regulates tumour suppressor p53 by counteracting Mdm2. β-arr2 nucleocytoplasmic shuttling displaces Mdm2 from the nucleus to the cytoplasm resulting in enhanced p53 signalling. β-arr2 is constitutively exported from the nucleus, via a nuclear export signal, but mechanisms regulating its nuclear entry are not completely elucidated. β-arr2 can be SUMOylated, but no information is available on how SUMO may regulate β-arr2 nucleocytoplasmic shuttling. While we found β-arr2 SUMOylation to be dispensable for nuclear import, we identified a non-covalent interaction between SUMO and β-arr2, via a SUMO interaction motif (SIM), that is required for β-arr2 cytonuclear trafficking. This SIM promotes association of β-arr2 with the multimolecular RanBP2/RanGAP1-SUMO nucleocytoplasmic transport hub that resides on the cytoplasmic filaments of the nuclear pore complex. Depletion of RanBP2/RanGAP1-SUMO levels result in defective β-arr2 nuclear entry. Mutation of the SIM inhibits β-arr2 nuclear import, its ability to delocalize Mdm2 from the nucleus to the cytoplasm and enhanced p53 signalling in lung and breast tumour cell lines. Thus, a β-arr2-SIM nuclear entry checkpoint, coupled with active β-arr2 nuclear export, regulate its cytonuclear trafficking function to control the Mdm2-p53 signalling axis.

Abstract 217 words

Main body text 4463 words

Introduction

Initially discovered for the roles they play in the regulation of G protein-coupled receptors (GPCRs), the β-arrestins (β-arr1 and β-arr2) have now been shown to act as scaffolding hubs that control multiple signalling pathways (1-3). Through their scaffolding properties β-arrs dynamically regulate the activity and/or subcellular distribution of non-GPCR protein partners such as ERK1/2 (4, 5) JNK3 (6), Mdm2 (7-9), PTEN (10-12) and FAK (13). While strong sequence homology exists between β-arr1 and β-arr2 they display different subcellular distributions (9, 14). Whereas β-arr1 is found in both the nucleus and cytoplasm at steady state, β-arr2 shows an apparent cytoplasmic distribution. We previously showed that β-arr2 is constitutively excluded from the nucleus by a leptomycin B-sensitive pathway driven by a nuclear export signal (NES) that is absent in β-arr1 (14). We also found that β-arr2 is actively imported into the nucleus, indicating that it undergoes constitutive nucleocytoplasmic shuttling (14). β-arr2 shuttling displaces nuclear partners, such as JNK3 and Mdm2, from the nucleus to the cytoplasm (9, 14). In the case of Mdm2, its β-arr2-mediated delocalization results in increased p53 signalling and cell cycle arrest (7). In contrast to the well characterized nuclear export mechanism of β-arr2 the entry mechanism(s) of β-arr2 into the nucleus are not completely elucidated.

β-arr2 can be SUMOylated (15, 16), but no information is available on how SUMO may regulate β-arr2 nucleocytoplasmic trafficking. SUMOylation is a key dynamic regulatory post-translational modification that impacts the activity and localization of protein targets including into the nucleus (17-19). These functional consequences are generally due to modification in protein-protein interactions caused by SUMOylation. Akin to the situation with the ubiquitination pathway, SUMOylation involves a series of sequential enzymatic reactions ultimately leading to covalent conjugation of the 12kDa protein SUMO on a lysine residue contained within a SUMOylation site (ψ-K-X-E; ψ, a bulky aliphatic residue, typically L, I or V) on a target protein (17, 18, 20). There are four SUMO isoforms in mammals: SUMO1, SUMO2 and SUMO3 are expressed ubiquitously, whereas SUMO4 displays tissue restricted expression and it is not clear whether it is conjugated to cellular proteins (21). SUMO2 and SUMO3 display 97% homology and contain internal SUMOylation sites allowing them to form poly-SUMO chains. SUMO1 shares 45% homology with SUMO2/3 (17). SUMOylation is reversible with SUMO-modified targets being subject

to cleavage of the isopeptide bond by SUMO-specific proteases that release SUMO molecules that become available for further SUMOylation cycles. SUMOylated proteins can establish non-covalent interaction with protein partners via SUMO interaction motifs (SIMs). Identified via two-hybrid screening and biophysical studies SIMs are composed of a short stretch of hydrophobic residues (generally V/I-V/I-X-V/I) flanked N- or C-terminally by serine residues and/or several acidic residues (17, 22). When bound to SUMO, SIMs adopt a parallel or antiparallel β-strand conformation that permits the hydrophobic side chains of the SIM to interact with a hydrophobic pocket on the surface of SUMO. The acidic flanking residues in the SIM form electrostatic interactions with a basic interface on SUMO, and thus also contribute to the SUMO-SIM interaction. SIMs can be involved in *cis*-SUMOylation or in recruitment/targeting of SIM-containing proteins to SUMOylated partners (17).

Using various *in vitro* and cell-based approaches we have characterized both a SUMOylation site and SIM in human β-arr2. Whereas β-arr2 SUMOylation is not required for nuclear import, mutation of the SIM prevents β-arr2 nuclear import. The SIM promotes association of β-arr2 with the multimolecular RanBP2/RanGAP1-SUMO nucleocytoplasmic transport hub and depletion of this complex inhibits β-arr2 nuclear import. The β-arr2ΔSIM mutant loses its ability to delocalize Mdm2 from the nucleus to the cytoplasm with functional consequences for p53 activity. Combined, our data reveal that a SUMO-SIM nuclear entry checkpoint, coupled with the nuclear export function of β-arr2, cooperate to regulate its cytonuclear trafficking function and subsequent control of the Mdm2-p53 pathway.

Results

Human β-arr2 is SUMOylated at lysine 295

To investigate the potential role of SUMO in the nucleocytoplasmic trafficking action of β-arr2 we first searched for potential SUMOylation sites within human β-arr2. Ubc9 fusion-directed SUMOylation (UFDS) experiments (23), which permit efficient and selective protein SUMOylation, were conducted by cloning the E2 conjugase Ubc9 coding sequence upstream of the open reading frame of β-arr2 with a C-terminal FLAG-tag, generating a coding sequence for a Ubc9-β-arr2-FLAG fusion protein (**Fig. 1a**). The fusion protein was expressed in HeLa cells in the presence of HA-SUMO1 or HA-SUMO2. Immunoprecipitations of the protein extracts using anti-FLAG antibodies followed by western blotting with anti-FLAG antibodies revealed the presence of a molecular weight (MW) band of ~100kDa corresponding to the Ubc9-β-arr2-FLAG fusion conjugated with HA-SUMO1 or HA-SUMO2 (**Fig. 1b and c**, lanes 2). The fused Ubc9 catalysed SUMOylation of β-arr2, as the active site mutant Ubc9C93S fused to β-arr2 (**Fig. 1a**) failed to promote β-arr2 SUMOylation in the presence of either SUMO1 or SUMO2 (**Fig. 1b and c**, lanes 3). Similar results were obtained with the fusions in β-arr1/2 knockout (KO)-mouse embryonic fibroblasts (**Fig. S1**). The expected MW of native β-arr2 is 55kDa. Following highly denaturing lysis, affinity pulldown with Ni-NTA resin greatly enriched SUMOylated human β-arr2 with a MW of ~75kDa corresponding to β-arr2 covalently conjugated with one molecule of SUMO2 in HEK-293 cells expressing exogenous native β-arr2, Ubc9 and His-SUMO2, or FLAG-tagged β-arr2, Ubc9 and His-SUMO2 (**Fig. 1d and Fig. 1e,** right lanes). SUMOylated β-arr2 was not observed in control cells lacking His-SUMO2 (**Fig. 1d and Fig. 1e,** left lanes). Similar results were obtained using a yellow fluorescent protein (YFP)-tagged form of β-arr2 (**Fig. 1f**, MW band at ~100kDa).

Human β-arr2 is a 409 amino acid protein composed of N- and C- globular domains linked together by a short hinge region, and a flexible regulatory C-terminal tail (**Fig. 2a**). To screen for a SUMO acceptor site(s) in β-arr2, a library of overlapping peptides (25-mers), each shifted by 5 amino acids across the entire sequence of β-arr2 (**Fig. 2a**), was SPOT-synthesized on cellulose membranes. The peptide arrays were subjected to *in vitro* SUMOylation assays using a SUMO assay mix containing

recombinant forms of E1-activase, E2-conjugase Ubc9, SUMO1, SUMO2 and SUMO3, and Mg-ATP solution. Control arrays were performed using SUMO assay mixtures that omitted Ubc9. The arrays were then probed with anti-SUMO antibodies and SUMOylated peptides were identified as dark spots. Using this approach, three consecutive SUMOylated peptides were identified comprising amino acids T276-G310 (**Fig. 2b and Fig. S2a**) that was absent in the control arrays. These peptides contained a consensus SUMOylation motif in β-arr2 294-L-K-H-E-297 that has previously been documented (15, 16). Confirming that K295 is indeed SUMOylated in the peptides, its mutation to alanine in a "progeny" 25-mer containing amino acids 276-300 inhibited SUMOylation (**Fig. 2c and Fig. S2b**). To confirm the SUMO acceptor site in cells, HEK-293 cells were co-transfected with YFP-β-arr2 or mutant YFP-β-arr2K295R in the presence of Myc-Ubc9 and His-SUMO2. While a ~100kDa band of SUMOylated YFP-β-arr2 was observed in Ni-NTA experiments in cells expressing wild-type β-arr2 (**Fig. 2d**, lane 1), this band was lost with the YFP-β-arr2K295R mutant (**Fig. 2d**, lane 2), consistent with this being a major SUMOylation site for β-arr2. Taken together, the above findings indicate that β-arr2 is SUMOylated both *in vitro* and in cells, and that K295, located in the regulatory "lariat loop" of the C-domain of β-arr2 (**Fig. 2e**), represents a major SUMO conjugation site contained within a consensus SUMOylation site.

Human β-arr2 contains a SIM in its N-domain

In addition to SUMOylation sites for covalent SUMO conjugation on lysine residues, SIMs exist that mediate non-covalent interaction between SUMO and SIM-containing proteins. We used a Joined Advanced Sumoylation Site and SIM Analyzer (JASSA) programme (24), which predicts SIMs, to analyse the primary sequence of β-arr2. A potential SIM was predicted in the N domain of β-arr2 between amino acids 41 and 44: 41-V-V-L-V-44 (**Fig. 3a and b**). **Figure 3a** shows the alignment of the potential SIM sequence in β-arr2 against other known SIMs found in Daxx, RanBP2, PML-III and PIAS1. In addition, the sequence in β-arr2 also contains two aspartic acid residues juxtaposed to the hydrophobic core (**Fig. 3a and b**), another important feature of functional SIMs. To test whether the potential SIM in β-arr2 is capable of non-covalent interaction with SUMO, we carried out pulldown experiments using SUMO1 and SUMO2 proteins coupled to agarose beads. Whereas wild-type β-arr2 bound to both SUMO1 and SUMO2 beads, a β-arr2ΔSIM mutant with the 41-V-V-L-

V-44 sequence mutated to 41-A-A-L-A-44 displayed greatly decreased binding (**Fig. 3c**). Thus, the SIM domain in β-arr2 is functional and provides non-covalent interaction with both SUMO1 and SUMO2.

β-arr2 SIM is required for nuclear import

β-arr2 is actively imported into the nucleus and subsequently excluded from the nuclear compartment via active nuclear export (14). As SUMOylation and non-covalent SUMO interactions are both known to impact protein targeting to the nucleus, we next investigated their possible involvement in the coordination of β-arr2 nucleocytoplasmic trafficking. HeLa cells were transfected with YFP-tagged forms of wild-type β-arr2, SUMOylation mutant (β-arr2K295R) or SIM mutant (β-arr2ΔSIM) (**Fig 4a**). The cells were then incubated with vehicle or Leptomycin B (LMB), a drug that specifically inhibits nuclear export of proteins containing leucine-rich nuclear export signals (NES) through inactivation of CRM1/exportin1 (25). All fusions demonstrated a cytoplasmic distribution at steady state (**Fig 4b**). As expected, a 1h incubation with LMB elicited wild-type β-arr2 nuclear accumulation (**Fig 4b**); β-arr2K295R also accumulated in the nucleus in the presence of LMB, demonstrating that SUMOylation on K295 is not required for nuclear import. In contrast, the β-arr2ΔSIM mutant failed to accumulate in the nucleus suggesting a default in its nuclear import. Similar results were obtained with non-tagged β-arr2ΔSIM, FLAG-tagged β-arr2ΔSIM and mCherry-tagged β-arr2ΔSIM (**Fig. S3**). Live cell imaging in cells transfected with YFP-tagged forms of β-arr2 corroborated results obtained in fixed cells: β-arr2 progressively accumulated in the nucleus during LMB incubation, whereas β-arr2ΔSIM did not (**Fig. 4c** and **d**), confirming that this mutant presents a defect in nuclear import. Despite this defect in nuclear import, control endocytosis experiments showed that β-arr2ΔSIM is still functional as it was able to promote internalization of the GPCR V2 vasopressin receptor (**Fig. S4a** and **b**).

SIMs can promote *in cis* SUMOylation of protein targets and this can occur on lysine residues that do not lie in strict consensus SUMOylation sequences (17). To rule out that potential additional minor SUMOylation on a secondary lysine in β-arr2 could contribute to nuclear import the β-arr2 primary sequence was analysed using the JASSA programme (24). In addition to the major K295 site, K11, K25, K53, K158, K293 and K400 were predicted as potential SUMOylation conjugation sites (**Fig. 5a**). We mutated these lysine residues to arginine either individually, or in combination

with the K295R mutation, and tested their impact on nuclear import by incubating HeLa cells expressing the mutant forms of β-arr2 with LMB for 1h. All mutants accumulated in the nucleus, like K295R, ruling out the possibility that they are implicated in nuclear import (**Fig. 5a** and **b**, and **Fig. S5**). Finally, we also created a SUMO1-β-arr2ΔSIM fusion tagged with YFP, to determine if SUMO fused to β-arr2ΔSIM could promote nuclear import. In the presence of LMB this fusion also failed to accumulate in the nucleus, in contrast to a fusion of β-arr2 with the nuclear localization signal (NLS) of SV40, which was able to rescue β-arr2ΔSIM nuclear import (**Fig. 5c**). We next tested the effect of the β-arr2ΔSIM mutation in a context where nuclear export of β-arr2 is inhibited through mutation of its NES (L394A). As expected YFP-β-arr2ΔNES strongly accumulated in the nucleus, however the ΔSIMΔNES mutant did not, again confirming the importance of the β-arr2 SIM in nuclear import (**Fig. 5d**). Similar results were obtained with fractionation experiments, showing marked enrichment of YFP-β-arr2ΔNES in the nuclear fraction, whereas YFP-β-arr2ΔSIMΔNES, like wild-type β-arr2, was not (**Fig. 5e**). We also used enhanced bystander bioluminescence resonance energy transfer (ebBRET), based on energy transfer between the naturally occurring chromophores luciferase (Rluc) and green fluorescent protein (rGFP) from Renilla (26) to monitor nuclear accumulation of β-arr2. For this, rGFP was targeted to the nucleus through fusion of an NLS (rGFP-NLS) and relative nuclear residency of Rluc-β-arr2 fusions were assessed by their ability to generate BRET signals (**Fig. 5f**). Rluc-β-arr2ΔNES generated a stronger BRET signal compared to wild-type in agreement with its expected nuclear localization (**Fig. 5f**). The ΔSIMΔNES mutant displayed a marked decrease in BRET compared to ΔNES indicating reduced nuclear accumulation.

The RanBP2/RanGAP1-SUMO complex gates β-arr2 nuclear entry

The above results indicate that whereas SUMOylation is not required for β-arr2 nuclear import, a non-covalent interaction of the β-arr2 SIM with a SUMOylated protein partner may contribute to its nuclear import. Interestingly, we found that β-arr2 associates with the nucleoporin RanBP2 and RanGAP1-SUMO1 (**Fig. 6a**), components of a multimolecular SUMO E3 ligase complex that resides on the cytoplasmic filaments of the nuclear pore complex. This complex is involved in substrate SUMOylation and acts as a hub for nucleocytoplasmic transport (27, 28). RanBP2 is a 358-kDa protein that contains multiple domains including several FG

repeats, four Ran-binding domains and a region that interacts with RanGAP1 (29) (30) (31) (32). The interaction of RanGAP1 with RanBP2 requires RanGAP1 SUMOylation (29). When the SIM in β-arr2 is mutated there is a marked reduction in coimmunoprecipitation of both RanGAP1-SUMO1 and RanBP2 with β-arr2, indicating the SIM is important for RanBP2 and RanGAP1-SUMO1 association with β-arr2 (**Fig. 6a**). To determine if RanBP2 may play a role in β-arr2 nuclear import we subjected HeLa cells to RanBP2 siRNA treatment and subsequently transfected the cells with mCherry-β-arr2ΔNES. Both RanBP2 and RanGAP1-SUMO1 levels were significantly reduced compared to control cells (**Fig. 6b**) as previously observed (33). Under these conditions Cherry-β-arr2ΔNES shifted from a nuclear to cytoplasmic distribution demonstrating that the RanBP2/RanGAP1-SUMO1 complex plays an important role in promoting β-arr2 nuclear import. These results indicate that the β-arr2 SIM targets β-arr2 to the RanBP2/RanGAP1-SUMO1 complex, which is involved in stimulation of β-arr2 nuclear entry.

Coordinated nuclear import and export of β-arr2 regulates Mdm2 subcellular localization and p53 activity

The nucleocytoplasmic shuttling function of β-arr2 displaces nuclear binding cargoes from the nucleus to the cytoplasm. It was previously demonstrated that displacement of Mdm2, the major negative regulator of p53, from the nucleus to the cytoplasm results in increased p53 activity (7). We anticipated that a functional SIM would be essential for Mdm2 displacement by β-arr2. In HEK 293 cells transfected with wild-type β-arr2, GFP-Mdm2 was displaced from the nucleus to the cytoplasm, unlike control cells, where GFP-Mdm2 remained nuclear (**Fig. 7a** and **b**). Quantification of Mdm2 displacement by β-arr2 demonstrated ~60% of Mdm2 cytoplasmic relocalization: in ~10% of cells Mdm2 was predominantly cytoplasmic and in ~50% partly cytoplasmic, in agreement with previous studies (7) (**Fig. 7c**). In the presence of β-arr2ΔSIM, the distribution of Mdm2 was similar to control Cherry/Mdm2 expressing cells (**Fig. 7a-c**). This indicates that due to defective nuclear import, β-arr2ΔSIM fails to displace Mdm2 from the nucleus to the cytosol. From a functional viewpoint with regard to Mdm2 displacement, the β-arr2ΔSIM therefore behaves like the β-arr2ΔNES mutant, which enters in the nucleus but cannot displace Mdm2 due to its defective nuclear export (**Fig. 7a-c**). The

SUMOylation K295R mutant of β-arr2 was still able to displace Mdm2 in line with its normal capacity to shuttle through the nucleus (**Fig. 7a-c**). Therefore, the SIM in β-arr2, coupled with its nuclear export function, combine to regulate β-arr2 cytonuclear trafficking function with consequences for Mdm2 subcellular localization.

To determine functional consequences of the defect in cytonuclear shuttling found with β-arr2ΔSIM on p53 signalling, we first used a H1299 non-small cell lung carcinoma cell line (p53-null) engineered to express p53 using the TETON system (34). We confirmed that the β-arr2ΔSIM defect in nuclear import was also found in these H1299-p53-TETON cells (**Fig. 8a**). We next transfected H1299-p53-TETON cells with a plasmid coding for luciferase under the control of multiple p53 response elements. As expected, incubation of the cells with doxycycline, to induce p53 expression comparative to endogenous levels found in MCF-7 breast cancer cells carrying *TP53* (**Fig. S6a**), robustly stimulated the luciferase signal, which was markedly reduced by exogenous Mdm2 (**Fig. 8b**). When β-arr2 was co-transfected with Mdm2, there was a significant increase in p53-dependent luciferase activity compared to Mdm2 alone. However, with the β-arr2ΔSIM mutant, which is defective in displacing Mdm2 to the cytoplasm (**Fig. 7a-c**), no significant increase in p53-dependent activity was observed. This indicates that β-arr2ΔSIM failed to rescue Mdm2-mediated inhibition of p53 activity.

As an additional cancer cell model, we used MCF-7 cells with endogenous levels of β-arr2, SUMO1, SUMO2, Ubc9, RanBP2, SUMO-RanGAP, Mdm2 and p53 (**Fig. S6b**) to investigate the effect of β-arr2ΔSIM versus wild-type β-arr2 on p53 signalling. We observed a similar defect in β-arr2ΔSIM nuclear import in MCF-7 cells (**Fig. 8c**), to that documented in HeLa, HEK and H1299-p53-TETON cells. Finally, we performed p53-dependent gene reporter experiments in MCF-7 cells. An enhancing effect on p53 signalling by wild-type Rluc-tagged β-arr2, expressed at comparative levels to endogenous β-arr2 **(Fig. S6c)**, was observed **(Fig. 8d)** and this effect was lost with β-arr2ΔSIM. Taken together, the above data therefore demonstrate the importance of the SIM in β-arr2 for enhancing p53 function in different cancer cell types.

Discussion

Mdm2 is the principal negative regulator of p53. Investigating mechanisms underlying Mdm2 regulation is therefore important in understanding p53 biology. β-arr2 nucleocytoplasmic shuttling serves to titrate Mdm2 from the nucleus to the cytoplasm to enhance p53 signalling (7). Under steady-state conditions this is a receptor-independent signalling mode of β-arr2. While the active nuclear export mechanism of β-arr2, due to the presence of a NES in its C-terminal tail, has been well characterized (9, 14), the mechanism(s) involved in its nuclear import are not completely elucidated. Previous studies have suggested that the N-domain is likely to play an important role in β-arr2 nuclear import (9, 14). Here, we demonstrate that SUMO orchestrates β-arr2 cytonuclear traffic. Whereas β-arr2 SUMOylation is not required for β-arr2 nuclear import, a SIM in the N-terminus of β-arr2 is involved in its nuclear import. Mutation of the SIM inhibits β-arr2 association with the RanBP2/RanGAP1-SUMO1 nucleocytoplasmic transport hub, and β-arr2 nuclear import. As a consequence, the ability of β-arr2 to titrate Mdm2 from the nucleus to the cytoplasm and effect on p53 signalling is impaired. Our data therefore unveil that a SUMO-SIM nuclear entry checkpoint, coupled with the nuclear export function of β-arr2, regulates its cytonuclear trafficking function to control the Mdm2-p53 loop.

We confirmed that K295 is a major SUMOylation site in human β-arr2. Previous studies of β-arr2 SUMOylation have shown that bovine β-arr2 is SUMOylated on both lysines K295 and K400 but that K400 represents the main SUMOylation site in this species (15). Inhibition of bovine β-arr2 SUMOylation, decreased its association with the endocytic partner β2-adaptin and attenuated β2-AR endocytosis (15). These data suggest that β-arr2 SUMOylation enhances its binding to β2-adaptin to promote the canonical function of β-arr2 in GPCR endocytosis. Alignment of the bovine and human sequences around K400, however, demonstrates that the human sequence does not fit a strict consensus SUMOylation site here. A subsequent study using human β-arr2 demonstrated that, in contrast to bovine β-arr2, the main SUMOylation site resides at K295 (16). SUMOylation on this site was found to inhibit β-arr2 binding to TRAF6, permitting enhanced TRAF6 oligomerization and autoubiquitination, and promoting TRAF6-mediated NF-κB signalling (16). Our results therefore agree with the study on human β-arr2 and confirm K295 as a main SUMOylation site. We found that SUMOylation of β-arr2,

however, was not essential for its nuclear import. This finding does not, however, rule out potential intranuclear roles for β-arr2 SUMOylation.

We also identified and characterized a SIM in the N-terminal domain of β-arr2 that we found was required for nuclear delivery. Similar to the role for the β-arr2 SIM in promoting nuclear delivery, SIMs have also been proposed to participate in the nuclear import/accumulation of several other proteins to date. These include the vaccinia virus protein E3 (35), the epstein-barr virus protein kinase BGLF4 (36), the viral restriction factor TRIM5α (37), and the MAPK p38 (38). This suggests that SIM-SUMO mediated transport may be a wider phenomenon involved in nuclear delivery of protein cargoes. SIMs promote recruitment/targeting of SIM-containing proteins to SUMOylated partners. For example, the transcriptional corepressor Daxx contains a SIM that is crucial for subnuclear targeting of Daxx to PML oncogenic domains and for the transrepression of several SUMOylated transcription factors (17, 39). Our results point towards a targeting role of the SIM in β-arr2 to RanBP2/RanGAP-SUMO1, which forms part of a SUMO E3 ligase complex, localized at the cytoplasmic nuclear pore complex (40). It is involved in the SUMOylation of certain substrates including Ran-GDP (27) and provides a hub for nucleocytoplasmic transport (28). A study investigating a nuclear import enhancement role by RanBP2 analyzed the distribution of approximately 200 nuclear proteins following RanBP2 depletion (28). The vast majority did not change subcellular distribution upon RanBP2 depletion, but around 5% were clearly affected, demonstrating cytoplasmic accumulation due to defective nuclear import. RanBP2 can therefore act as a platform for nuclear import for a subset of import cargos (28). Our results demonstrating cytoplasmic accumulation of β-arr2ΔNES following RanBP2 depletion clearly indicate that this nucleoporin is required for β-arr2 nuclear entry. It was proposed that RanBP2 can enhance nuclear import by at least two mechanisms. First, it reduces the active concentration of import receptors required for efficient transport (41, 42) and second import receptor-independent interaction of selected cargos with RanBP2 can increase efficiency of nuclear import (28). This suggests that β-arr2 nuclear import probably involves multiple steps coordinated by RanBP2. Indeed, a recent study identified a nuclear localization signal in β-arr2 and importin β1-dependent nuclear import (43). This suggests that β-arr2 has dual nuclear entry signals similar to what has been documented with the nuclear protease Calpain 5 (44). RanBP2 serves as a binding site for importin β1 keeping the transport receptor in association with the

nuclear pore complex. RanBP2 therefore likely acts as a hub to coordinate spatiotemporal regulation of β-arr2 nuclear import occurring through dual nuclear entry motifs. In summary, our findings demonstrate that the β-arr2 SIM targets it to the RanBP2/RanGAP-SUMO1 complex, which gates β-arr2 nuclear entry.

As mutation of the SIM inhibits β-arr2 nuclear import, its ability to delocalize Mdm2 from the nucleus to the cytoplasm and effect on enhanced p53 signalling is impaired. The ΔSIM mutant therefore gives rise to the same impaired p53 signalling effect as the ΔNES mutant, which also fails to displace Mdm2 from the nucleus (7). Our results uncovering the critical role of a β-arr2 SIM in its nuclear entry, coupled with the previously characterized export mechanism, generate an emerging picture of regulatory nodes that impact receptor-independent β-arr2-mediated control of the Mdm2/p53 axis. Future studies will be required to determine if β-arr2 cytonuclear shuttling function is altered in cancer settings.

Materials and Methods

Reagents, plasmids and antibodies.

A full list of reagents, plasmids and antibodies is provided in the Supplementary Materials and Methods section.

Cell culture and transfection

Cell culture and transfection conditions are provided in the Supplementary Materials and Methods section.

His-tagged protein purification using Ni-NTA beads

Assay conditions for His-tagged protein purification are provided in the Supplementary Materials and Methods section

SUMO beads pulldown assay

For isolation and enrichment of SUMO interacting proteins, SUMO agarose beads from ENZO were used. Assay conditions are provided in the Supplementary Materials and Methods section.

SPOT synthesis of peptides

A peptide library of overlapping 25-mers, that scan the entire human β-arr2 sequence, was produced by automatic SPOT synthesis and synthesized on continuous cellulose membrane supports on Whatman 50 cellulose membranes using Fmoc (fluoren-9-ylmethoxycarbonyl) chemistry with the AutoSpot-Robot ASS 222 (Intavis Bioanalytical Instruments), as described previously (45).

In vitro SUMOylation on β-arr2 peptide arrays

A SUMOylation kit (Biomol) was used according to the manufacturer's instructions for the SUMOylation of putative SUMO sites contained within the β-arr2 peptide array (46). The SUMO assay mix was incubated with array membranes at 30°C with shaking. Membranes were washed with TBS-T (Tris-buffered saline with Tween 20: 137mM NaCl, 20mM Tris/HCl, pH7.6, and 0.1% Tween 20) followed by probing the SUMOylated moities on the peptide array using an anti-SUMO antibody.

Control arrays were performed using SUMO assay mixtures that omitted the E2 conjugase Ubc9.

Coimmunoprecipitation

HEK cells were transiently transfected with plasmids as indicated in the figure legends and following lysis subjected to coimmunoprecipitation as detailed in the Supplementary Materials and Methods section.

Live cell imaging and Immunofluorescence

Live cell imaging and immunofluorescence experiments were conducted as previously described (47). Details are provided in the Supplementary Materials and Methods section.

Flow Cytometry

The details of the flow cytometry assay used to monitor β-arr2-dependent endocytosis of HA-V2R-vYFP have been described previously (48). Details are provided in the Supplementary Materials and Methods section.

Cytoplasmic and nuclear fractionation

Cytoplasmic and nuclear extracts were prepared from HeLa cells using the Invent Biotechnologies Minute^{TM} fractionation kit according to the manufacturer's instructions.

Enhanced bystander bioluminescence resonance energy transfer (ebBRET)

Endocytosis and nuclear localization ebBRET assays were performed in HEK cells and are described in the Supplementary Materials and Methods section.

Gene reporter experiments

H1299-p53-TETON cells and MCF-7 cells were co-transfected with p53-luc (Stratagene), containing 14xp53-response elements, and either pRL.TK (H1299 cells) or Rluc-tagged forms of β-arr2 (MCF-7 cells) using Lipo3000 in 12-well plates. Cells were lyzed using passive lysis buffer (Promega) and both firefly and Renilla luciferase activities detected using the Dual-Luciferase Reporter Assay System (Promega).

Molecular Modelling

The 3D structure used for β-arr2 is PDB:3P2D (Zhan et al., 2011). Figures were prepared with PyMol Molecular Graphics System, Version 2.0 Schrödinger, LLC.

Data analysis and statistics

Data are represented as mean ± s.e.m. Statistical analysis was performed using GraphPad Prism using unpaired *t*-tests or one-way analysis of variance with Tukey's *post-hoc* test.

Acknowledgements

We thank Drs A. Benmerah for helpful discussion, J. Liotard for excellent technical assistance, and the Institut Cochin Imaging (IMAG'IC) and Sequencing platforms (GENOM'IC). The Institut Cochin lab is part of the Who am I? laboratory of excellence (grant ANR-11-LABX-0071), funded by the “Investments for the Future” program operated by The French National Research Agency (grant ANR-11-IDEX-0005-01). This work was funded by grants from the Fondation ARC pour la Recherche sur le Cancer ("Projet ARC" to M.G.H.S.), Ligue contre le Cancer (to M.G.H.S.), Royal Society ("International Joint Project Scheme" to M.G.H.S. and G.S.B.), France Canada Research Fund (to M.G.H.S. and S.A.), CNRS and INSERM. E.B.T was funded by MESR and Fondation ARC pour la Recherche sur le Cancer doctoral fellowships.

Author contributions

EBT, ML, BS, JSP, GSB, HE, MB, SA, SM and MGHS designed research. EBT, ML, JSP, BS, MK, KS, JF, AP and MGHS performed research. EBT, ML, BS, JSP, CA, ELF, AZ, LG, GSB, HE, MB, SA, SM and MGHS analyzed data. MGHS supervised the project. EBT and MGHS wrote the manuscript, which was subsequently reviewed by all other authors.

The authors declare that they have no conflict of interest.

References

1. Enslen H, Lima-Fernandes E, Scott MG. Arrestins as regulatory hubs in cancer signalling pathways. Handb Exp Pharmacol. 2014;219:405-25.
2. Laporte SA, Scott MGH. beta-Arrestins: Multitask Scaffolds Orchestrating the Where and When in Cell Signalling. Methods Mol Biol. 2019;1957:9-55.
3. Peterson YK, Luttrell LM. The Diverse Roles of Arrestin Scaffolds in G Protein-Coupled Receptor Signaling. Pharmacol Rev. 2017;69(3):256-97.
4. Luttrell LM, Roudabush FL, Choy EW, Miller WE, Field ME, Pierce KL, et al. Activation and targeting of extracellular signal-regulated kinases by beta-arrestin scaffolds. Proc Natl Acad Sci U S A. 2001;98(5):2449-54.
5. Luttrell LM, Wang J, Plouffe B, Smith JS, Yamani L, Kaur S, et al. Manifold roles of beta-arrestins in GPCR signaling elucidated with siRNA and CRISPR/Cas9. Sci Signal. 2018;11(549).
6. McDonald PH, Chow CW, Miller WE, Laporte SA, Field ME, Lin FT, et al. Beta-arrestin 2: a receptor-regulated MAPK scaffold for the activation of JNK3. Science. 2000;290(5496):1574-7.
7. Boularan C, Scott MG, Bourougaa K, Bellal M, Esteve E, Thuret A, et al. beta-arrestin 2 oligomerization controls the Mdm2-dependent inhibition of p53. Proc Natl Acad Sci U S A. 2007;104(46):18061-6.
8. Shenoy SK, McDonald PH, Kohout TA, Lefkowitz RJ. Regulation of receptor fate by ubiquitination of activated beta 2- adrenergic receptor and beta-arrestin. Science. 2001;294(5545):1307-13.
9. Wang P, Wu Y, Ge X, Ma L, Pei G. Subcellular localization of beta-arrestins is determined by their intact N domain and the nuclear export signal at the C terminus. J Biol Chem. 2003;278:11648-53.
10. Javadi A, Deevi RK, Evergren E, Blondel-Tepaz E, Baillie GS, Scott MG, et al. PTEN controls glandular morphogenesis through a juxtamembrane beta-Arrestin1/ARHGAP21 scaffolding complex. Elife. 2017;6.
11. Lima-Fernandes E, Enslen H, Camand E, Kotelevets L, Boularan C, Achour L, et al. Distinct functional outputs of PTEN signalling are controlled by dynamic association with beta-arrestins. Embo J. 2011;30(13):2557-68.

12. Lima-Fernandes E, Misticone S, Boularan C, Paradis JS, Enslen H, Roux PP, et al. A biosensor to monitor dynamic regulation and function of tumour suppressor PTEN in living cells. Nat Commun. 2014;5:4431.
13. Alexander RA, Lot I, Saha K, Abadie G, Lambert M, Decosta E, et al. Beta-arrestins operate an on/off control switch for focal adhesion kinase activity. Cell Mol Life Sci. 2020.
14. Scott MG, Le Rouzic E, Perianin A, Pierotti V, Enslen H, Benichou S, et al. Differential nucleocytoplasmic shuttling of beta-arrestins. Characterization of a leucine-rich nuclear export signal in beta- arrestin2. J Biol Chem. 2002;277(40):37693-701.
15. Wyatt D, Malik R, Vesecky AC, Marchese A. Small ubiquitin-like modifier modification of arrestin-3 regulates receptor trafficking. J Biol Chem. 2011;286(5):3884-93.
16. Xiao N, Li H, Mei W, Cheng J. SUMOylation attenuates human beta-arrestin 2 inhibition of IL-1R/TRAF6 signaling. J Biol Chem. 2015;290(4):1927-35.
17. Flotho A, Melchior F. Sumoylation: a regulatory protein modification in health and disease. Annual review of biochemistry. 2013;82:357-85.
18. Geiss-Friedlander R, Melchior F. Concepts in sumoylation: a decade on. Nat Rev Mol Cell Biol. 2007;8(12):947-56.
19. Hay RT. SUMO: a history of modification. Mol Cell. 2005;18(1):1-12.
20. Rodriguez MS, Dargemont C, Hay RT. SUMO-1 conjugation in vivo requires both a consensus modification motif and nuclear targeting. J Biol Chem. 2001;276(16):12654-9.
21. Guo D, Li M, Zhang Y, Yang P, Eckenrode S, Hopkins D, et al. A functional variant of SUMO4, a new I kappa B alpha modifier, is associated with type 1 diabetes. Nat Genet. 2004;36(8):837-41.
22. Kerscher O. SUMO junction-what's your function? New insights through SUMO-interacting motifs. EMBO Rep. 2007;8(6):550-5.
23. Jakobs A, Koehnke J, Himstedt F, Funk M, Korn B, Gaestel M, et al. Ubc9 fusion-directed SUMOylation (UFDS): a method to analyze function of protein SUMOylation. Nat Methods. 2007;4(3):245-50.
24. Beauclair G, Bridier-Nahmias A, Zagury JF, Saib A, Zamborlini A. JASSA: a comprehensive tool for prediction of SUMOylation sites and SIMs. Bioinformatics. 2015;31(21):3483-91.

25. Kudo N, Matsumori N, Taoka H, Fujiwara D, Schreiner EP, Wolff B, et al. Leptomycin B inactivates CRM1/exportin 1 by covalent modification at a cysteine residue in the central conserved region. Proc Natl Acad Sci U S A. 1999;96(16):9112-7.

26. Namkung Y, Le Gouill C, Lukashova V, Kobayashi H, Hogue M, Khoury E, et al. Monitoring G protein-coupled receptor and beta-arrestin trafficking in live cells using enhanced bystander BRET. Nat Commun. 2016;7:12178.

27. Sakin V, Richter SM, Hsiao HH, Urlaub H, Melchior F. Sumoylation of the GTPase Ran by the RanBP2 SUMO E3 Ligase Complex. J Biol Chem. 2015;290(39):23589-602.

28. Walde S, Thakar K, Hutten S, Spillner C, Nath A, Rothbauer U, et al. The nucleoporin Nup358/RanBP2 promotes nuclear import in a cargo- and transport receptor-specific manner. Traffic. 2012;13(2):218-33.

29. Mahajan R, Delphin C, Guan T, Gerace L, Melchior F. A small ubiquitin-related polypeptide involved in targeting RanGAP1 to nuclear pore complex protein RanBP2. Cell. 1997;88(1):97-107.

30. Matunis MJ, Wu J, Blobel G. SUMO-1 modification and its role in targeting the Ran GTPase-activating protein, RanGAP1, to the nuclear pore complex. J Cell Biol. 1998;140(3):499-509.

31. Wu J, Matunis MJ, Kraemer D, Blobel G, Coutavas E. Nup358, a cytoplasmically exposed nucleoporin with peptide repeats, Ran-GTP binding sites, zinc fingers, a cyclophilin A homologous domain, and a leucine-rich region. J Biol Chem. 1995;270(23):14209-13.

32. Yokoyama N, Hayashi N, Seki T, Pante N, Ohba T, Nishii K, et al. A giant nucleopore protein that binds Ran/TC4. Nature. 1995;376(6536):184-8.

33. Hashizume C, Kobayashi A, Wong RW. Down-modulation of nucleoporin RanBP2/Nup358 impaired chromosomal alignment and induced mitotic catastrophe. Cell Death Dis. 2013;4:e854.

34. Monteith JA, Mellert H, Sammons MA, Kuswanto LA, Sykes SM, Resnick-Silverman L, et al. A rare DNA contact mutation in cancer confers p53 gain-of-function and tumor cell survival via TNFAIP8 induction. Mol Oncol. 2016;10(8):1207-20.

35. Gonzalez-Santamaria J, Campagna M, Garcia MA, Marcos-Villar L, Gonzalez D, Gallego P, et al. Regulation of vaccinia virus E3 protein by small ubiquitin-like modifier proteins. J Virol. 2011;85(24):12890-900.
36. Li R, Wang L, Liao G, Guzzo CM, Matunis MJ, Zhu H, et al. SUMO binding by the Epstein-Barr virus protein kinase BGLF4 is crucial for BGLF4 function. J Virol. 2012;86(10):5412-21.
37. Brandariz-Nunez A, Roa A, Valle-Casuso JC, Biris N, Ivanov D, Diaz-Griffero F. Contribution of SUMO-interacting motifs and SUMOylation to the antiretroviral properties of TRIM5alpha. Virology. 2013;435(2):463-71.
38. Wang PY, Hsu PI, Wu DC, Chen TC, Jarman AP, Powell LM, et al. SUMOs Mediate the Nuclear Transfer of p38 and p-p38 during Helicobacter Pylori Infection. Int J Mol Sci. 2018;19(9).
39. Lin DY, Huang YS, Jeng JC, Kuo HY, Chang CC, Chao TT, et al. Role of SUMO-interacting motif in Daxx SUMO modification, subnuclear localization, and repression of sumoylated transcription factors. Mol Cell. 2006;24(3):341-54.
40. Werner A, Flotho A, Melchior F. The RanBP2/RanGAP1*SUMO1/Ubc9 complex is a multisubunit SUMO E3 ligase. Mol Cell. 2012;46(3):287-98.
41. Hutten S, Flotho A, Melchior F, Kehlenbach RH. The Nup358-RanGAP complex is required for efficient importin alpha/beta-dependent nuclear import. Mol Biol Cell. 2008;19(5):2300-10.
42. Hutten S, Walde S, Spillner C, Hauber J, Kehlenbach RH. The nuclear pore component Nup358 promotes transportin-dependent nuclear import. J Cell Sci. 2009;122(Pt 8):1100-10.
43. Zhang X, Min X, Wang S, Sun N, Kim KM. Mdm2-mediated ubiquitination of beta-arrestin2 in the nucleus occurs in a Gbetagamma- and clathrin-dependent manner. Biochem Pharmacol. 2020;178:114049.
44. Singh R, Brewer MK, Mashburn CB, Lou D, Bondada V, Graham B, et al. Calpain 5 is highly expressed in the central nervous system (CNS), carries dual nuclear localization signals, and is associated with nuclear promyelocytic leukemia protein bodies. J Biol Chem. 2014;289(28):19383-94.
45. Bolger GB, Baillie GS, Li X, Lynch MJ, Herzyk P, Mohamed A, et al. Scanning peptide array analyses identify overlapping binding sites for the signalling scaffold proteins, beta-arrestin and RACK1, in cAMP-specific phosphodiesterase PDE4D5. Biochem J. 2006;398(1):23-36.

635 46. Li X, Vadrevu S, Dunlop A, Day J, Advant N, Troeger J, et al. Selective SUMO
636 modification of cAMP-specific phosphodiesterase-4D5 (PDE4D5) regulates the
637 functional consequences of phosphorylation by PKA and ERK. Biochem J.
638 2010;428(1):55-65.
639 47. Blondel-Tepaz E, Guilbert T, Scott MGH. Methods to Investigate the
640 Nucleocytoplasmic Shuttling Properties of beta-Arrestins. Methods Mol Biol.
641 2019;1957:251-69.
642 48. Paradis JS, Ly S, Blondel-Tepaz E, Galan JA, Beautrait A, Scott MG, et al.
643 Receptor sequestration in response to beta-arrestin-2 phosphorylation by ERK1/2
644 governs steady-state levels of GPCR cell-surface expression. Proc Natl Acad Sci U S
645 A. 2015;112(37):E5160-8.
646

Figure Legends

Figure 1. β-arr2 is SUMOylated in cells. (a) Schematic diagram details the Ubc9-β-arr2-FLAG and catalytically dead Ubc9C93S-β-arr2-FLAG UFDS fusions. **(b and c)** SUMOylation of β-arr2 assessed by UFDS. Ubc9-β-arr2 or Ubc9C93S-β-arr2 were coexpressed with HA-SUMO1 (**b**) or HA-SUMO2 (**c**) in HeLa cells as indicated. The protein extracts were subject to immunoprecipitation using EZview Red ANTI-FLAG® M2 Affinity Gel, and fusions and SUMOylated fusions were detected by western blot using anti-FLAG antibodies. The top set of arrows indicate SUMOylated forms of Ubc9-β-arr2. HEK-293T cells were co-transfected with plasmids encoding Ubc9, His-tagged SUMO2 or empty vector, and either **(d)** β-arr2, **(e)** β-arr2-FLAG or **(f)** YFP-β-arr2. 48h later, cells were lysed in denaturing conditions followed by purification on Ni-NTA beads. Cell lysates and His-SUMO conjugated proteins purified with Ni-NTA agarose beads were analyzed by western blot with the indicated antibodies. The arrow indicates SUMO2-conjugated β-arr2.

Figure 2. β-arr2 is SUMOylated on lysine 295. (a) Schematic diagram showing the library of overlapping 25-mer peptides that cover the entire β-arr2 sequence. **(b)** The peptide library was overlaid with SUMO conjugation assay mixture (Ubc9+) including recombinant His-SUMO1, His-SUMO2 and His-SUMO3. Dark spots represent a run of peptides that displayed successful conjugation of recombinant SUMO to immobilized peptides that are absent in the control array (Ubc9-). **(c)** Alanine substitution at K295 inhibits SUMO conjugation on the immobilized 276-300 peptide. **(d)** K295R mutation inhibits SUMOylation in cells following lysis in denaturing conditions and purification on Ni-NTA beads. **(e)** Structure of β-arr2 in cartoon representation, with SUMO site in red sticks representation (left), zoom on K295 residue (right).

Figure 3. β-arr2 contains a SIM in its N-domain (a) Alignment of the putative SIM sequence in the N-domain of β-arr2 against other known characterized SIMs in Daxx, RanBP2, PML-III and PIAS1. **(b)** Structure of β-arr2 in cartoon representation, with SIM site in orange sticks representation (left), zoom on the SIM residues, also highlighting the DPD loop in green sticks (right). **(c)** Pulldown of wild-type β-arr2 but not β-arr2ΔSIM mutant by SUMO1- or SUMO2-agarose beads.

Figure 4. The SIM but not SUMOylation on lysine 295 is required for β-arr2 nuclear entry. (a) Schematic diagram showing the SIM and K295 SUMOylation site in β-arr2. The SIM was mutated from 41-VVLV-44 to 41-AALA-44 and the SUMOylation site changed from 294-LKHE-297 to 294-LRHE-297. **(b)** HeLa cells transfected with YFP-tagged β-arr2 wild-type, β-arr2-K295R, or β-arr2ΔSIM were incubated with methanol control (CTL) or 20 nM LMB for 60 min at 37°C, then fixed and processed for confocal fluorescence microscopy. Representative images are shown. **(c)** Direct visualization of YFP-β-arr2 WT or YFP-β-arr2ΔSIM nuclear accumulation in live HeLa cells in the presence of 20 nM LMB for 60 min. Images were acquired using a spinning disk confocal microscope equipped with a 37°C heated control chamber. Images acquired every 15 min are displayed. **(d)** Quantification of β-arr2 WT or β-arr2ΔSIM nuclear accumulation in the presence of LMB in live cells. Fluorescence intensity was quantified using the previously described ImageJ plugin (Blondel et al., 2019) and values were plotted as a percentage of maximal WT response. Data represent mean ± s.e.m (n=10; ***$P<0.001$). Scale bars, 10 µm.

Figure 5. SUMO1 fusion to β-arr2ΔSIM does not rescue nuclear import but an NLS fusion does. (a) Schematic diagram showing other potential SUMOylation sites predicted by JASSA. **(b)** HeLa cells were transfected with the indicated constructs and incubated with 20 nM LMB for 60 min. Accumulation of the various fusions in the nucleus is indicated. **(c)** HeLa cells transfected with plasmids encoding YFP-SUMO1-β-arr2ΔSIM or YFP-NLS-β-arr2ΔSIM were incubated with methanol (vehicle control) or 20 nM LMB during 1 hour at 37 °C, then fixed and processed for fluorescence microscopy. **(d)** HeLa cells transfected with plasmids encoding YFP-β-arr2, YFP-β-arr2ΔNES, or YFP-β-arr2ΔSIMΔNES were subsequently fixed and processed for fluorescence microscopy. All cells were visualized on a confocal microscope. Representative images of all conditions are shown. Scale bars, 10 µm. **(e)** Nuclear and cytoplasmic fractions of HeLa cells, transfected with plasmids encoding YFP-β-arr2, YFP-β-arr2ΔNES, or YFP-β-arr2ΔSIMΔNES, were prepared. The fractions were analyzed by western blot. GAPDH was used as a cytoplasmic marker and p75 as a nuclear marker. **(f)** Schematic representation of the ebBRET system. The RlucII donor is fused to β-arr2, and the rGFP acceptor to a nuclear localization signal (NLS), to target it to the nucleus (see fluorescence panels). Changes in BRET signals

indicate changes in nuclear accumulation. HEK293 cells transfected with plasmids encoding β-arr2-RlucII, β-arr2-ΔNES-RlucII or β-arr2-ΔSIMΔNES-RlucII and rGFP-NLS were used to monitor relative β-arrestin2 nuclear localization by ebBRET. The inset shows equivalent expression of the different forms of β-arr2-RucII. Data represent mean ± s.e.m (n=5; **P<0.01, ns: non-significant).

Figure 6. The β-arr2 SIM enhances association with the RanBP2/RanGAP1-SUMO complex and RanBP2/RanGAP1-SUMO depletion inhibits β-arr2 nuclear entry. (a) Western blot of FLAG immunoprecipitates from HEK cells expressing β-arr2- FLAG or β-arr2ΔSIM-FLAG showing reduced association of β-arr2ΔSIM with RanGAP1-SUMO1 and RanBP2. Data shown represent the mean ± s.e.m. of five independent experiments (***P<0.001). **(b)** HeLa cells were transfected with control siRNA or siRNA targeting RanBP2. Quantification of western blots demonstrated knockdown of 85±1.6% for RanBP2, and 85±7.8% for RanGAP-SUMO1 (mean ± s.e.m., n=4). The cells were subsequently transfected with Cherry-β-arr2ΔNES and cytonuclear distribution visualized directly in live HeLa cells. Representative images are shown. Scale bars, 10 μm.

Figure 7. A functional SIM domain is required for β-arr2-mediated cytoplasmic delocalization of Mdm2. (a) HEK cells expressing mCherry, mCherry-β-arr2, mCherry-β-arr2ΔSIM, mCherry-β-arr2-K295R or mCherry-β-arr2ΔNES (left column) and GFP-Mdm2 constructs (middle column) were imaged using a spinning disk confocal microscope. Merged images are shown in the right column. Scale bar, 10 μm. **(b)** Line traces generated in ImageJ of the corresponding traces (white dotted lines) in the merged images shown in **(a)** with Cherry and GFP intensities displayed in red and green respectively. The blue area defines the nuclear area. **(c)** Manual quantification of nuclear (N), cytoplasmic (C), or partially displaced Mdm2 localization (N/C). Bars indicate the percentage of cells in each category. Over 100 cells were quantified for each experimental condition (***P<0.001, **P<0.01, ns: non-significant).

Figure 8. The β-arr2 SIM domain is required for increased p53 signalling

(a) H1299 cells expressing YFP-β-arr2 or YFP-β-arr2ΔSIM were treated with methanol control (CTL) or 20nM LMB for 60 minutes and live cells were imaged

directly using a spinning disk confocal microscope. Scale bar 10 µm. **(b)** H1299-p53-TETON cells were stimulated with 100ng/ml doxycycline to induce p53 expression (+p53) and subsequently transfected with 14xp53-RE-luc and control pRL.TK, in addition to the indicated combinations of empty vector (-), Mdm2 and β-arr2/β-arr2ΔSIM plasmids. Promoter activity driven by p53 is expressed as a ratio of firefly luciferase:Renilla luciferase activity. Equivalent expression of β-arr2 and β-arr2-ΔSIM is shown in the western blot inset. Data are expressed as mean ± s.e.m., n=3; **P<0.01. **(c)** MCF-7 cells expressing Cherry-β-arr2 or Cherry-β-arr2ΔSIM were treated with methanol control (CTL) or 20nM LMB for 60 minutes and live cells were directly imaged using a spinning disk confocal microscope. Scale bar 10 µm. **(d)** MCF-7 cells were transfected with 14xp53-RE-luc and either empty vector, Rluc-β-arr2 or Rluc-β-arr2ΔSIM. Equivalent luciferase expression of Rluc-β-arr2 or Rluc-β-arr2ΔSIM is shown in the inset. Data are expressed as mean ± s.e.m., n=4; **P<0.01.

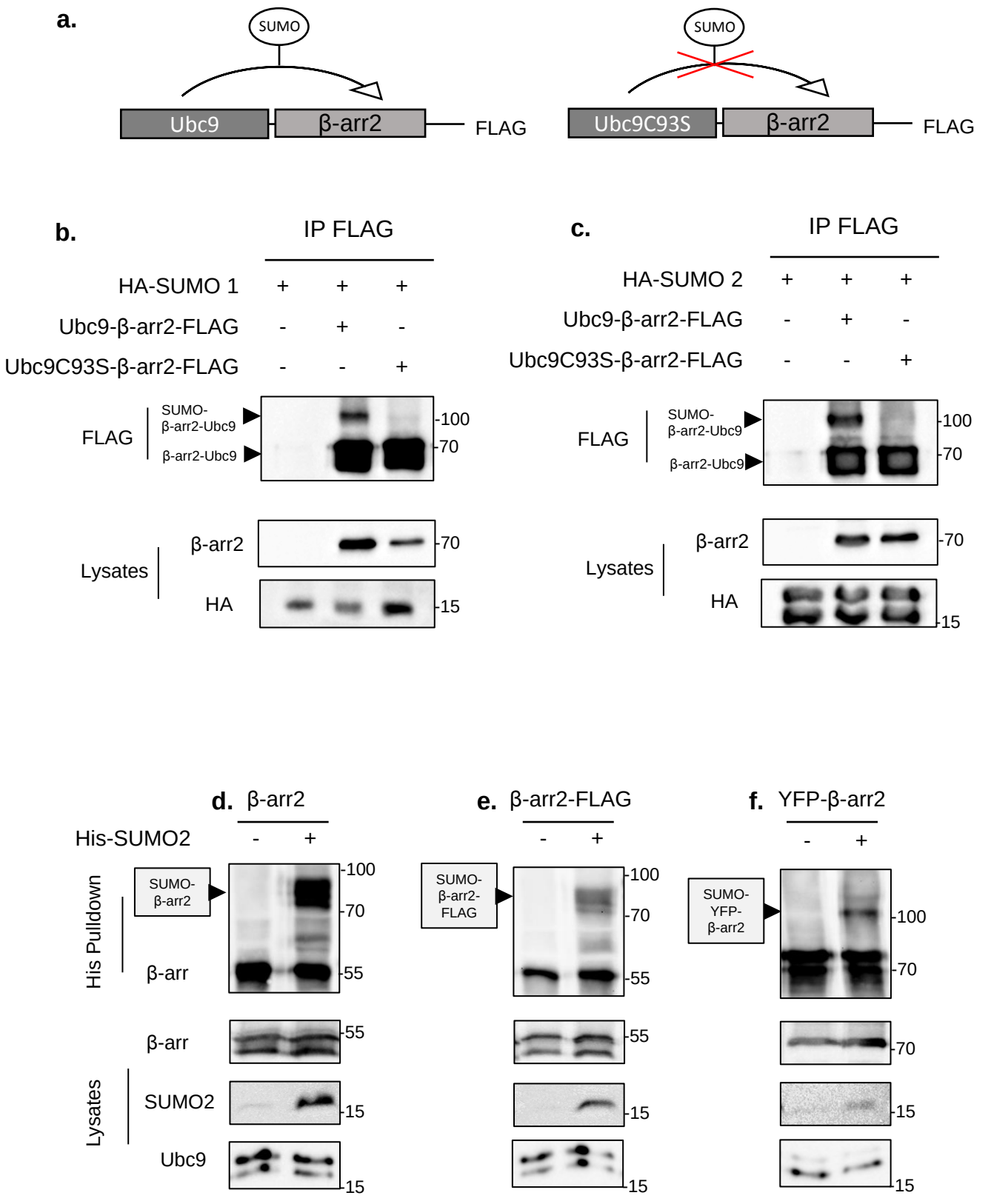

Blondel-Tepaz et al. Fig. 1

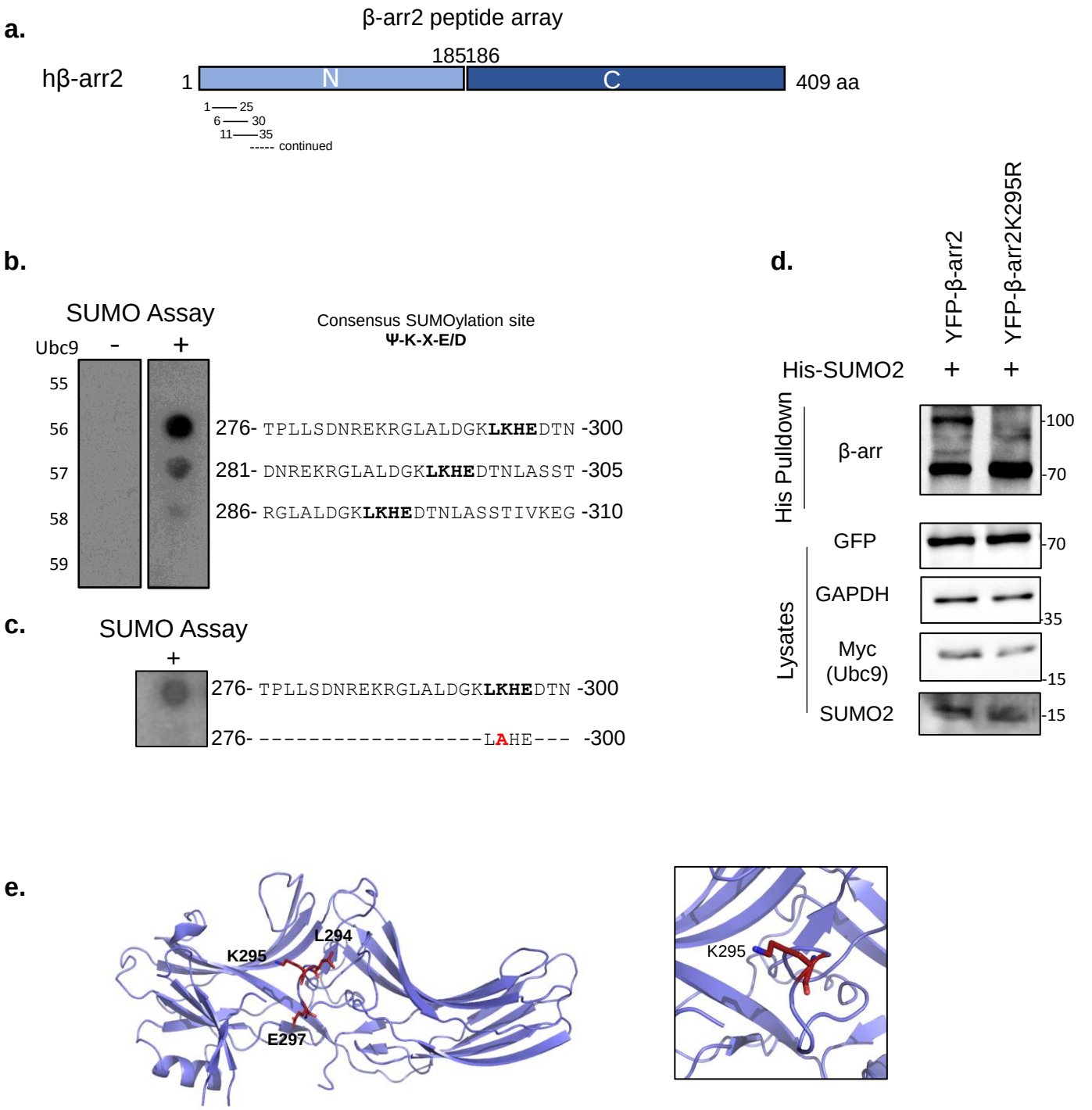

Blondel-Tepaz et al. Fig. 2

a.

Consensus SIM		:	**(V/I)-(V/I)-X-(V/I)**		
hβ-arr2	37	-	PVDG**VVLV**DPDY	-	48
Daxx	3	-	TANS**IIVL**DDDDEDE	-	17
	729	-	DPEE**IIVL**SDSD	-	740
Ran-BP2	2628	-	SDDD**VLIV**YELTPTAE	-	2643
PML-III	552	-	AEER**IIVL**SSSEDSD	-	566
PIAS1	455	-	KKVE**VIDL**TIDSSSDEEEEE	-	474

b.

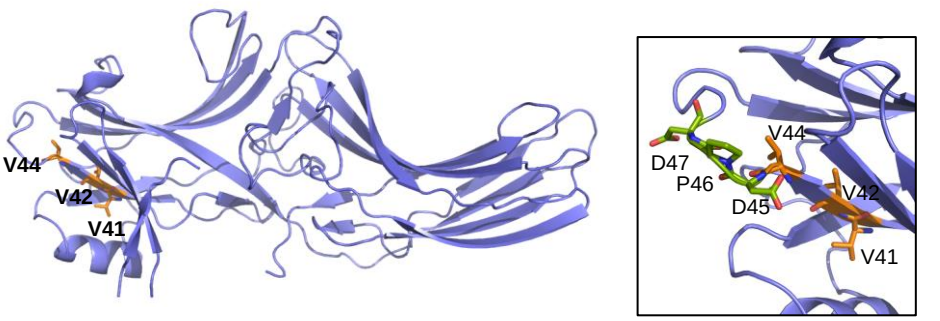

c.

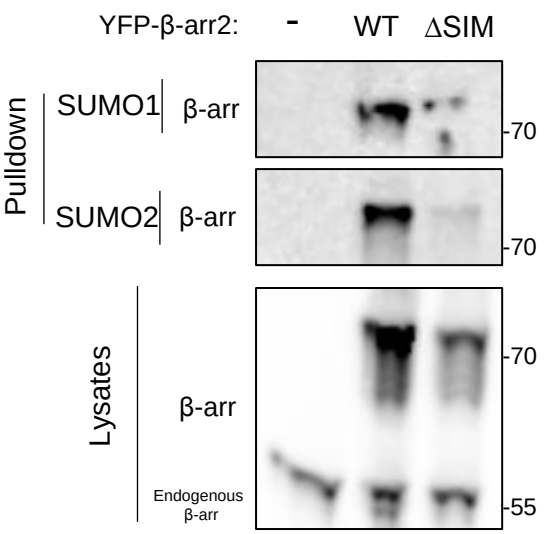

Blondel-Tepaz et al. Fig. 3

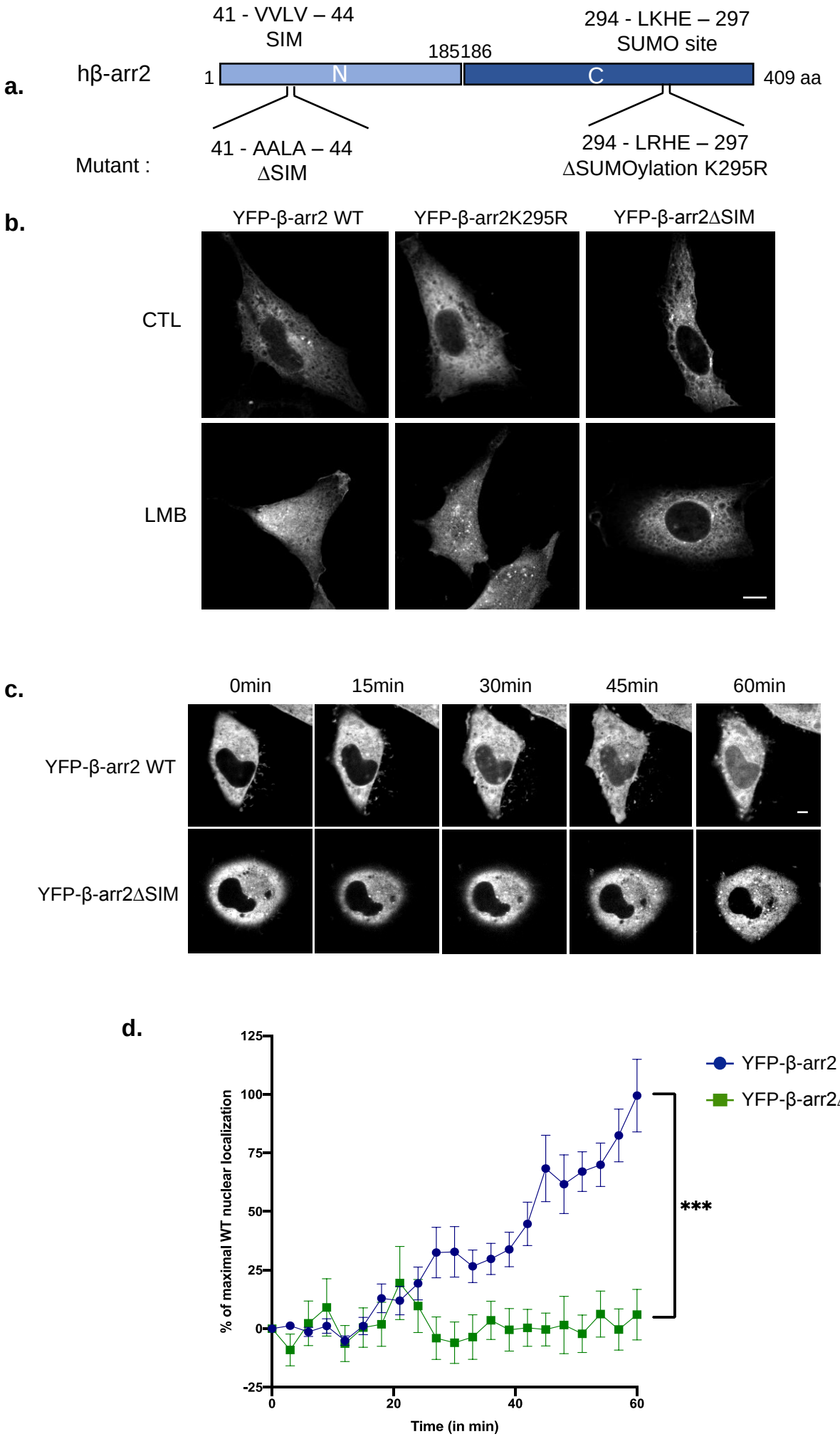

Blondel-Tepaz et al. Fig. 4

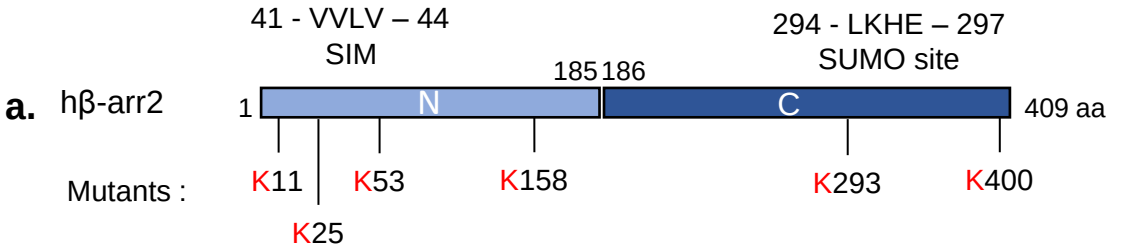

b.

		Nuclear distribution with LMB
Flag constructs	hβ-arr2K11R	+
	hβ-arr2K25R	+
	hβ-arr2K53R	+
	hβ-arr2K158R	+
	hβ-arr2K293R	+
	hβ-arr2K295R	+
	hβ-arr2K400R	+
	hβ-arr2K11R-K295R	+
	hβ-arr2K25R-K295R	+
	hβ-arr2K53R-K295R	+
	hβ-arr2K158R-K295R	+
	hβ-arr2K293R-K295R	+
	hβ-arr2K295R-K400R	+

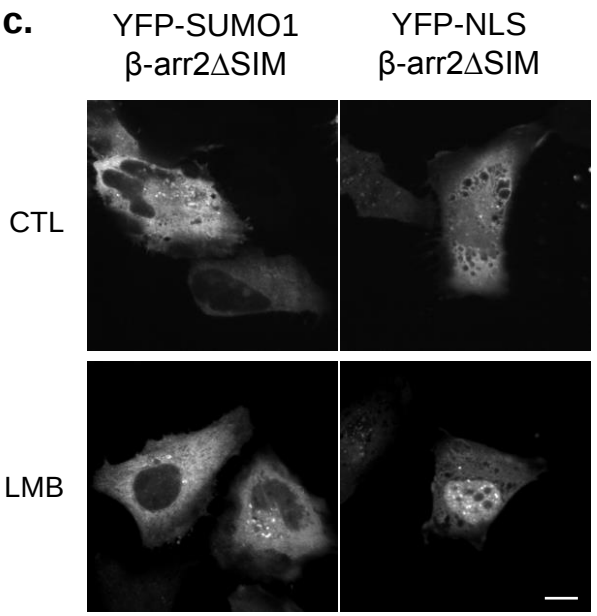

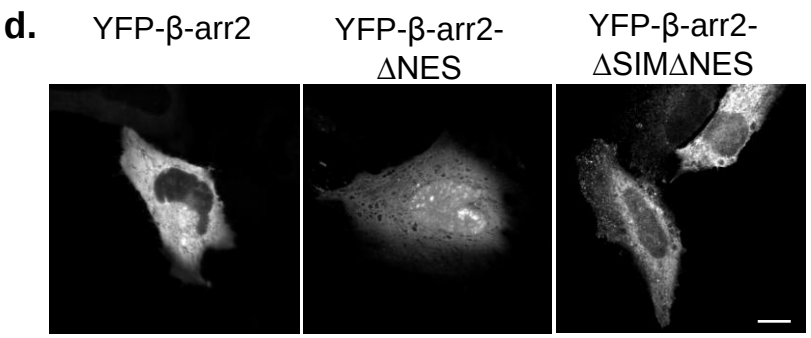

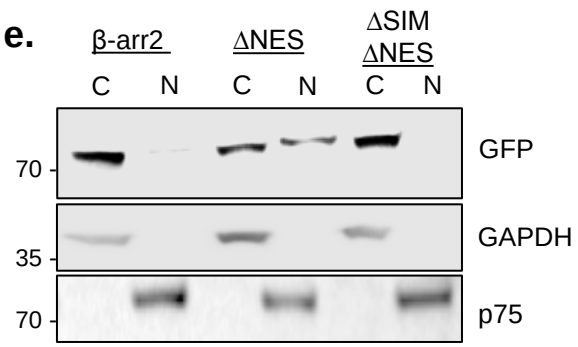

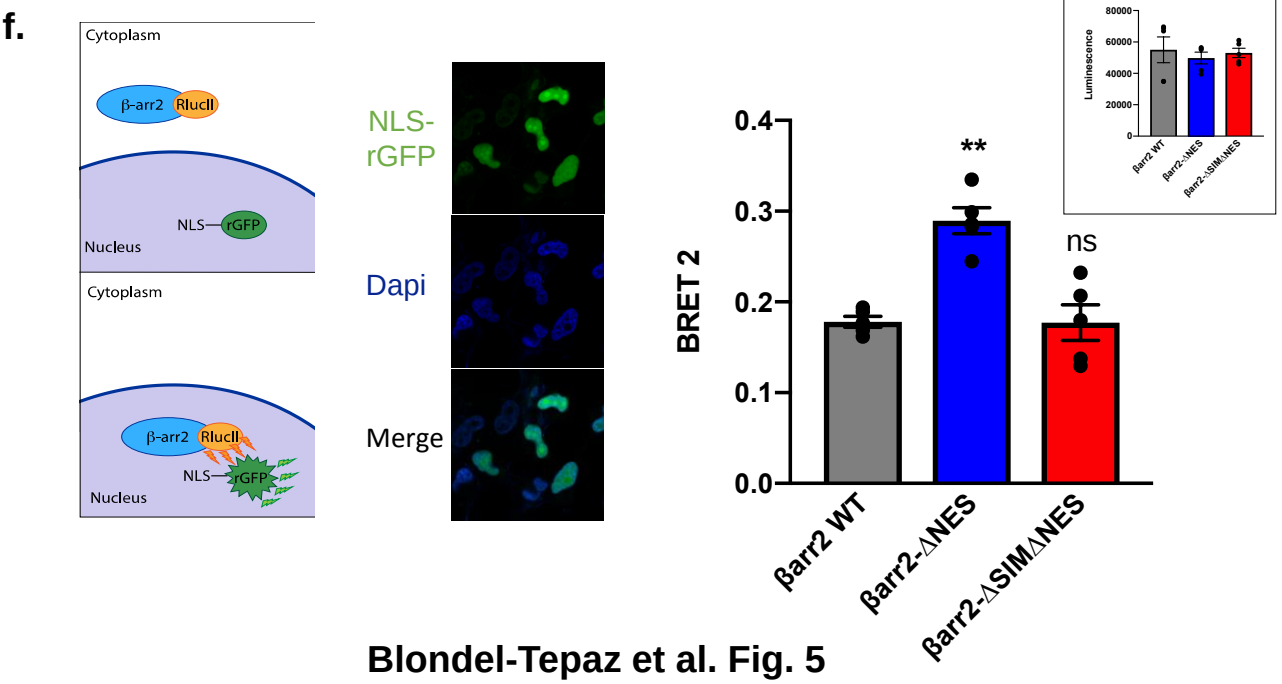

Blondel-Tepaz et al. Fig. 5

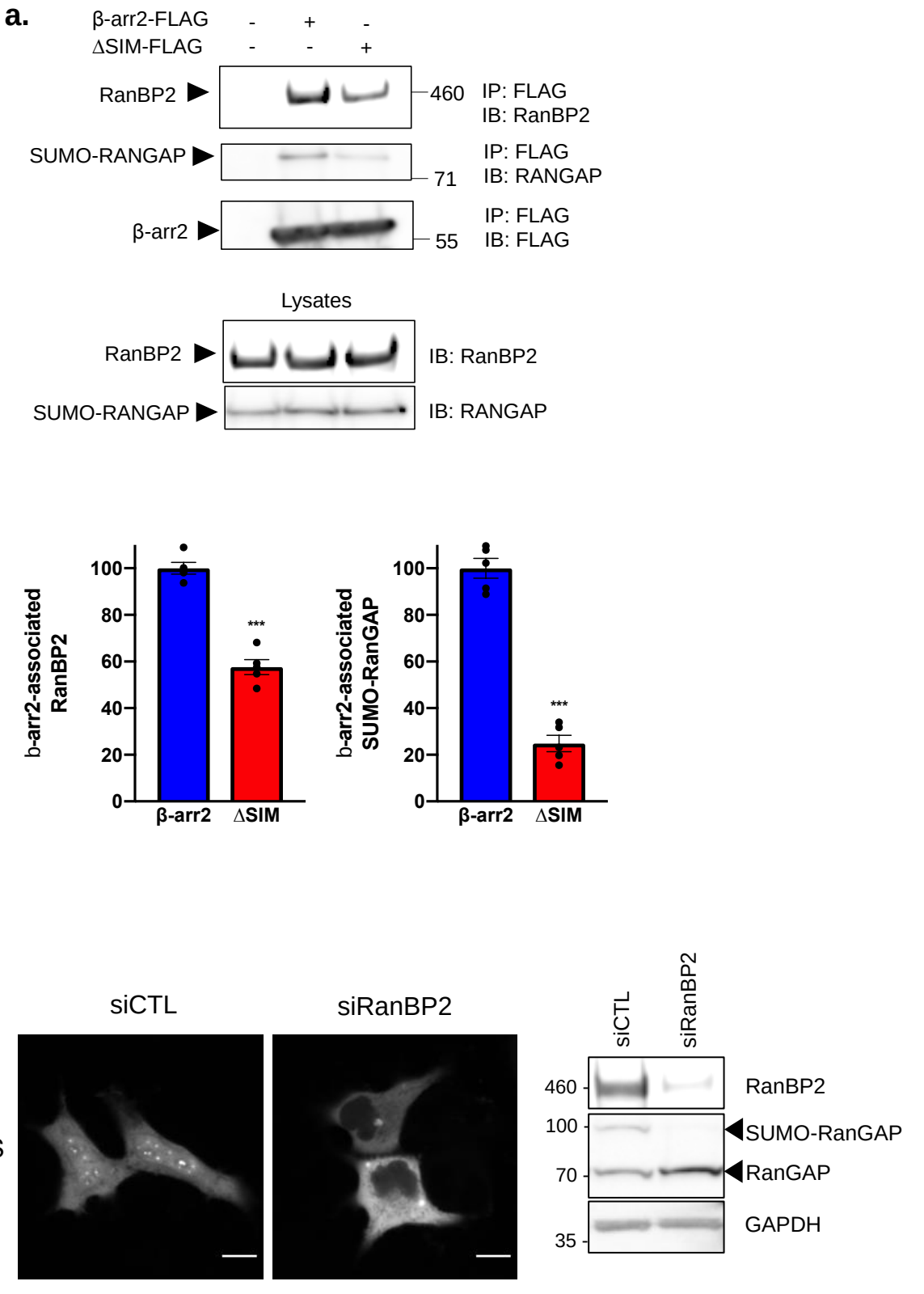

Blondel-Tepaz et al. Fig. 6

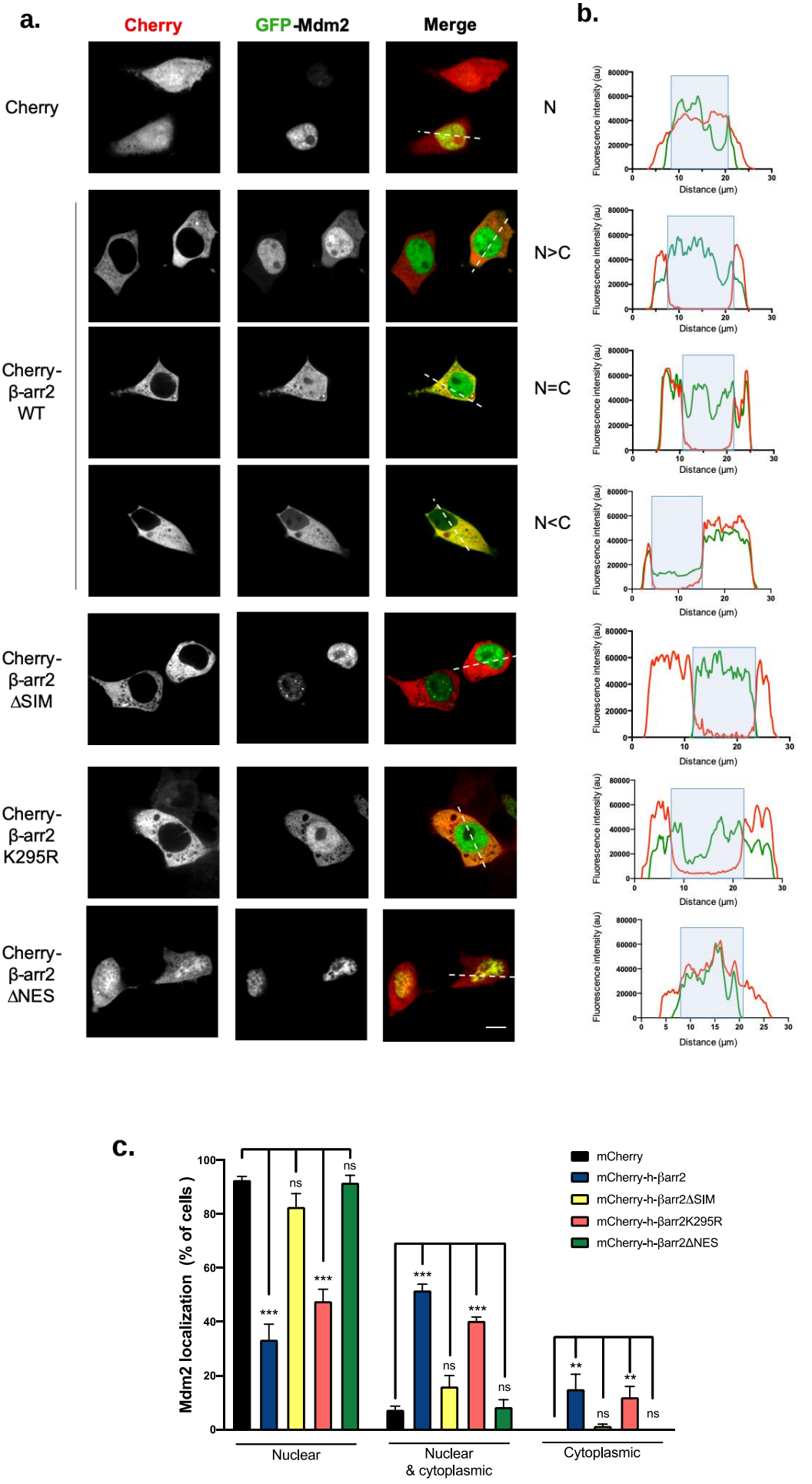

Blondel-Tepaz et al. Fig. 7

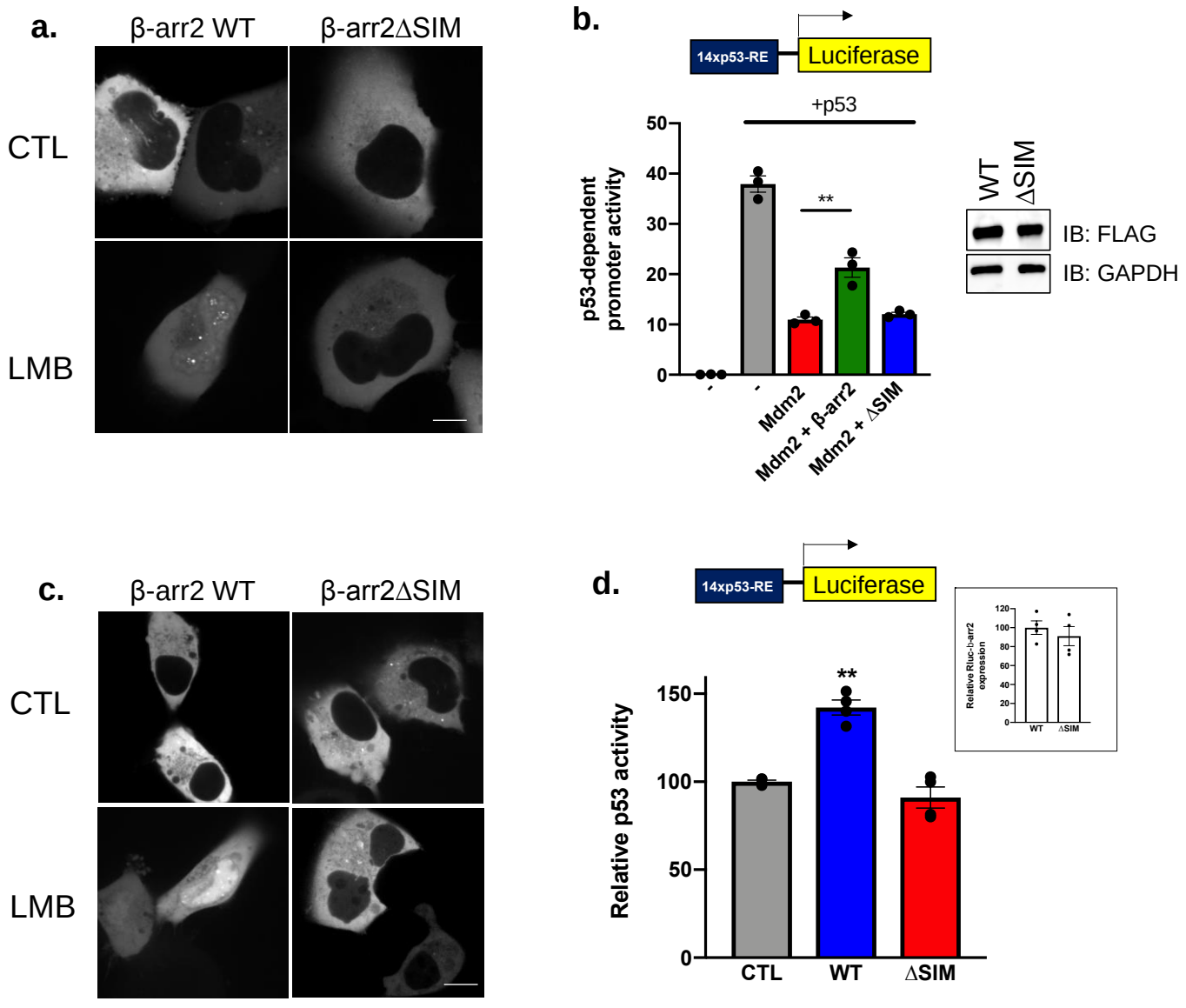

Blondel-Tepaz et al. Fig. 8